

quantum-mechanical estimates of the core size³¹ indicate that a varies as $m^{-1/2}$. Equations (71) and (74) then imply the curious result that a reduced value of m leads to a *reduced* mean-square displacement of the vortex axis. This effect may be understood by noting that the circulation κ in vortex dynamics is analogous to the inertial mass in Newtonian dynamics: An increase in κ decreases the zero-point motion. Unfortunately, these qualitative arguments are not directly applicable to the motion of quantized flux lines in type-II superconductors, because the frequency spectrum is greatly altered

³¹ E. P. Gross, *Nuovo Cimento* **20**, 454 (1961); L. P. Pitaevskii, *Zh. Eksperim. i Teor. Fiz.* **40**, 646 (1961) [English transl.: *Soviet Phys.—JETP* **13**, 451 (1961)].

from that studied here whenever the wavelength is larger than the penetration depth. The detailed theory of vortex dynamics in bulk type-II superconductors requires a separate treatment and will be presented in a subsequent paper.

ACKNOWLEDGMENTS

This work originated in conversations with Professor D. S. Falk and Professor R. A. Ferrell. It has benefited from comments and suggestions by Professor F. Bloch and D. Stauffer, for which I am most grateful. I should also like to thank D. Stauffer for sending me his unpublished results [Eq. (44)].

Lambda Curve of Liquid He⁴†

HENRY A. KIERSTEAD

Argonne National Laboratory, Argonne, Illinois

(Received 27 April 1967)

We have measured the pressure P_λ and the derivatives $(dP/dT)_\lambda$ and $(d\rho/dT)_\lambda$ of the lambda curve of He⁴ as a function of temperature from the upper lambda point to the lower lambda point, using an apparatus of very high resolution. Empirical equations for P_λ and ρ_λ are presented which represent our data very well and agree generally with previous measurements. These equations define the position and slope of the lambda curve in the ρ , P , T space to a higher order of accuracy and detail than has been possible before.

I. INTRODUCTION

THE application of Pippard's¹ relations or the methods of Buckingham and Fairbank² to the lambda transformation of He⁴, requires a knowledge of various thermodynamic derivatives along the lambda curve, such as $(dP/dT)_\lambda$ and $(d\rho/dP)_\lambda$. However, the values of these derivatives are not known with sufficient accuracy, since the pressure and density of the lambda transformation have not been measured at small enough temperature intervals to permit accurate differentiation.

The present experiment was designed to measure the derivatives $(dP/dT)_\lambda$ and $(d\rho/dP)_\lambda$ directly at many points along the lambda curve. The resolution of the apparatus was about 1 μ deg K in temperature, 10^{-5} atm in pressure, and better than 10^{-8} g/cm³ in density. With this resolution it was no problem to make measurements over such small intervals that curvature corrections were negligible.

The slope $(dP/dT)_\lambda$ of the lambda curve at the point where it meets the vapor-pressure curve (the lower lambda point) is needed for the correlation of heat-

capacity measurements with thermal-expansion and sound-velocity measurements at the lower lambda point. Many values have been quoted, ranging from -80 to -130 atm/deg. We have made a special effort to obtain a reliable value for this slope.

While this experiment was in progress, Elwell and Meyer³ reported measurements of the lambda density and pressure at 22 temperatures and the slope $(dP/dT)_\lambda$ at 11 temperatures. Their results are in general agreement with ours, as will be seen later.

II. EXPERIMENTAL

The apparatus used in these experiments is similar to that used previously.⁴⁻⁶ It is shown schematically in Fig. 1.

Helium gas was purified in a trap (not shown) immersed in liquid helium and was condensed into the sample compartment G through the low-temperature valve A, which has kept closed during measurements. G was isolated from the liquid helium bath by the

† Based on work performed under the auspices of the U. S. Atomic Energy Commission.

¹ A. B. Pippard, *Phil. Mag.* **1**, 473 (1956).

² M. V. Buckingham and W. M. Fairbank, *Progress in Low-Temperature Physics*, edited by J. C. Gorter (North-Holland Publishing Company, Amsterdam, 1961), Vol. 3, p. 80.

³ D. L. Elwell and H. Meyer, *Bull. Am. Phys. Soc.* **11**, 175 (1966); *Proceedings of the Conference on Low-Temperature Physics, Moscow, 1966* (to be published); *Phys. Rev.* (to be published); H. Meyer (private communication).

⁴ H. A. Kierstead, *Phys. Rev.* **138**, A1594 (1965).

⁵ H. A. Kierstead, *Phys. Rev.* **144**, 166 (1966).

⁶ H. A. Kierstead, *Phys. Rev.* **153**, 258 (1967).

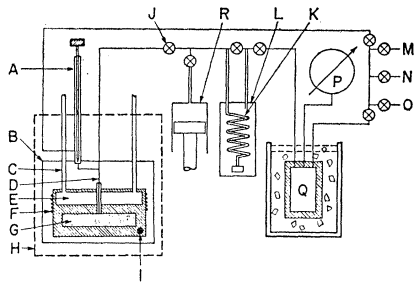


FIG. 1. Schematic drawing of the apparatus. (A) needle valve; (B) vacuum case; (C) pumping and vapor pressure tubes (2) for (E); (D) 30% Cu-Ni capillary tubing; (E) temperature and vapor pressure compartment; (F) heater; (G) sample compartment packed with fine copper wire for rapid equilibrium (volume 41.72 cm³ at 1.76°K, height 10 mm to keep hydrostatic-pressure differences small); (H) dashed lines enclose space immersed in liquid helium bath; (I) germanium thermometer; (J) needle valve used as density control; (K) quartz Bourdon tube; (L) reference capsule; (M) to He⁴ supply tank and purifier; (N) to pump; (O) to atmosphere; (P) 35-cm dial test gauge calibrated against a dead-weight tester; (Q) ballast volume (1461 cm³) for balancing the right-hand side of K, held at constant temperature by an ice bath; (R) volumetric micrometer; ⊗ needle valves.

vacuum case B. Its temperature was controlled by the heater F and by pumping on liquid helium in E.

For measurements above 3.2 atm, the absolute pressure of the sample was read to 0.01 atm on the stainless-steel Bourdon gauge⁷ P, which was calibrated against a dead-weight tester after the experiment. Pressure changes were measured by means of the differential quartz-helix Bourdon gauge⁸ K with a stainless-steel high-pressure reference capsule L. The reference pressure was maintained constant by connecting the reference capsule to a large reservoir Q of helium gas in a well-stirred ice bath. The quartz Bourdon tube and reference capsule were filled with Apiezon B oil, and the stainless-steel Bourdon tube was filled with mercury, in order to reduce the dead space. It was necessary to correct for changes in temperature of the small volumes of gas in the dead space at room temperature and at the Bourdon gauge temperature. A correction was also made for thermal expansion of the oil in the Bourdon gauge. The gauge was sensitive to pressure changes of 10⁻⁶ atm, but the precision of the pressure measurements was limited to about 10⁻⁵ atm by uncertainty of the dead-space corrections to the reference pressure. This gauge was calibrated against a dibutylphthalate manometer read to ±0.02 mm with a cathetometer.

For measurements below 3.4 atm, K was a 3.4-atm quartz-helix Bourdon gauge⁹ with the reference capsule connected to the vacuum system. The reservoir Q and the stainless-steel Bourdon gauge were not used. The quartz Bourdon gauge had a resolution of 10⁻⁵ atm.

⁷ Heise Bourdon Tube Company, 35-cm dial, 1000 lb/in.² graduated at 1-lb/in.² intervals.

⁸ Texas Instruments, Inc., Model 140, capsule type 4, Bourdon tube No. 14 (0-75 mm Hg).

⁹ Capsule type 1, Bourdon tube No. 3 (0-3.4 atm).

The manufacturer's calibration was used for this gauge. It was checked against a mercury manometer up to atmospheric pressure and was found to be accurate to better than 0.1%. Both pressure measuring systems were used at 3.35 atm. The results were in good agreement with each other for differential pressures, but not for absolute pressures (see below).

The capillary tube connecting the sample compartment to the pressure gauge was vacuum jacketed within the cryostat. It was made of copper down to a point 5 cm above the top of the vacuum case B. From this point to the sample compartment, the tubing was 30% copper-nickel. It was thermally anchored to the top of the vacuum case, which was kept at 4.2°K by the liquid He bath. The copper tubing was 1.6 mm o.d. by 0.51 mm i.d. and the copper-nickel tubing was 0.51 mm o.d. by 0.10 mm i.d. in the experiments above 3.2 atm. In the experiments below 3.4 atm the copper tube was 2.1 mm o.d. by 0.79 mm i.d. and the copper-nickel tubing was 0.51 mm o.d. × 0.28 mm i.d. Nearly all of the 300°K temperature drop from room temperature to the bath temperature was across the 5-cm length of copper-nickel capillary, so the liquid level in the capillary remained at a point very close to the top of the vacuum case, except when the pressure was below 1 atm. A small correction was made for the head of liquid in the capillary. It was never more than 0.0014 atm and was nearly constant in experiments above 1 atm.

No attempt was made to measure absolute densities. For each experiment, the cell was filled to the desired pressure through the low-temperature valve A. For measuring $(d\rho/dP)_\lambda$ the density was changed in small increments by displacing He gas from the room-temperature part of the apparatus. Since the gas density increases with pressure while $(d\rho/dP)_\lambda$ decreases, much greater gas volumes were needed for the lower pressures than for higher pressures. Therefore, two different calibrated displacement systems were used. At pressures between 9 and 30 atm, sufficient density change was obtained by turning the stem of valve J in and out. It was provided with a dial plate calibrated in degrees. It had a resolution of 10⁻⁵ cm³ of gas and a range of 0.09 cm³. From 2 to 14.6 atm the displacement was provided by a volumetric micrometer consisting of a cylinder with an O-ring-sealed piston driven by a precision screw and a gear box, and provided with a counter. Its resolution was 2 × 10⁻⁴ cm³/count and its range was 14 cm³. This instrument was also used to calibrate the valve J, whose dimensions could not be measured with sufficient accuracy. Both methods of measuring density changes were used between 9 and 14.6 atm. The results were in good agreement with each other.

Temperatures were measured with a Radiation Research Corporation series CG-1 germanium resistance thermometer in an AC potentiometer circuit, using a seven-dial Gertsch Model 1011R ratio transformer as

the balancing element and a Princeton Applied Research Corporation Model CR-4A low-noise amplifier and Model JB-4 lock-in amplifier as null detector. The measuring current was obtained from a Hewlett-Packard Model 204B audio oscillator. The frequency was about 300 cps. The measuring circuit is shown in Fig. 2. The temperature resolution was about $1 \mu\text{deg}$ at the upper lambda point and about $2 \mu\text{deg}$ at the lower lambda point.

The resistance thermometer was calibrated against the vapor pressure of He in E on the T_{58} scale,¹⁰ through a measuring tube separate from the pumping tube. We believe that our temperature scale agrees with the T_{58} scale to better than 10^{-4} °K in absolute temperature, and to one part per thousand for temperature differences.

The lambda transformation was observed in the following way. With the sample below the lambda temperature, the heater current was adjusted so that the sample temperature increased at a rate of about 10^{-5} deg/min, at constant density, and the temperature was plotted on a strip chart recorder. Because of the abrupt change in thermal conductivity at the lambda transformation, the heating curve showed a sharp break, which could be located to within a microdegree. The sample was then held at the lambda temperature until pressure equilibrium was established, and the lambda-point pressure was recorded. Then the density was changed by means of valve J or the volumetric micrometer, and the new lambda temperature and pressure were observed in the same way. The reference pressure was kept constant for a series of such measurements so that the high resolution of the differential quartz Bourdon gauge could be utilized.

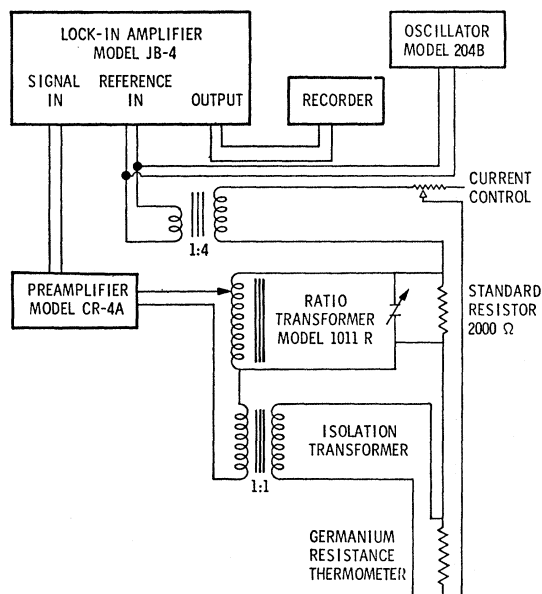


Fig. 2. Alternating current potentiometer circuit for germanium resistance thermometer.

For the density change provided by the total range of the valve J or of the volumetric micrometer, the change in pressure was sufficiently large compared to the resolution of the pressure measurements that accurate values of $(d\rho/dP)_\lambda$ could be obtained at all pressures greater than 0.64 atm. However, the temperature change was often less than $100 \mu\text{deg}$. Therefore, $(dP/dT)_\lambda$ was measured in separate experiments in which the pressure was changed by bleeding He out of the low-temperature valve. In these experiments the intervals were limited

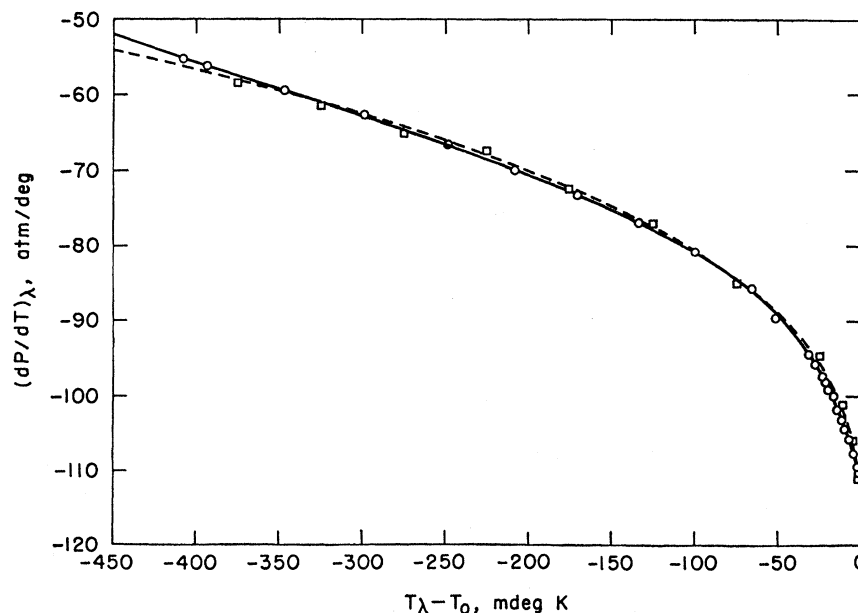


Fig. 3. Slope of the lambda curve; \circ this work, \square Elwell and Meyer (Ref. 3). Solid line represents Eq. (1), dashed line represents Eq. (2).

¹⁰ H. Van Dijk, M. Durieux, J. R. Clement, and J. K. Logan, Natl. Bur. Std. U. S., Mon. 10, 1 (1960).

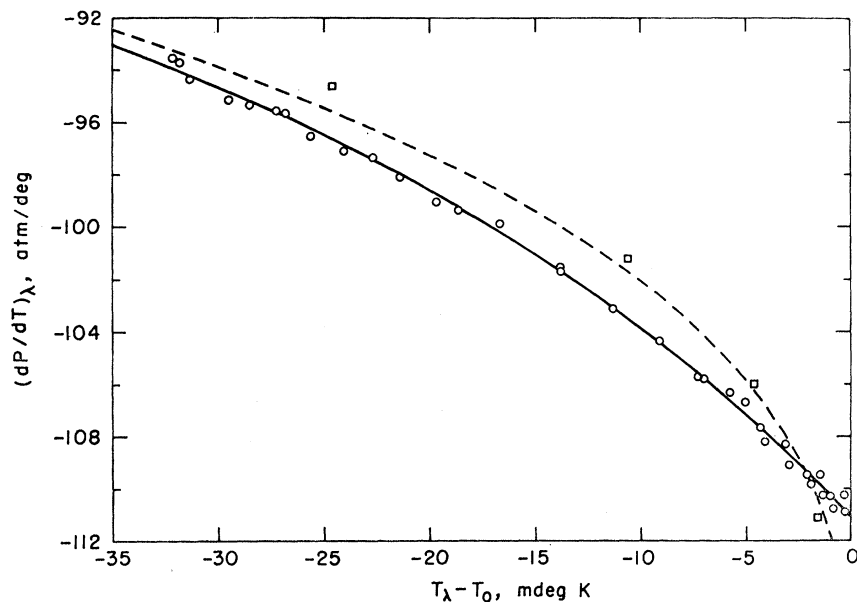


FIG. 4. Slope of the lambda curve near the lower lambda point; \circ this work, \square Elwell and Meyer (Ref. 3). Solid line represents Eq. (1), dashed line represents Eq. (2).

only by the 0.1-atm range of the differential Bourdon gauge.

In all cases the intervals were sufficiently small that curvature corrections to the derivatives $(dP/dT)_\lambda$ and $(d\rho/dP)_\lambda$ were negligible.

III. LAMBDA PRESSURES

In Fig. 3 are shown the results of 47 measurements of $(dP/dT)_\lambda$, plotted against $T_\lambda - T_0$. Here T_λ is the lambda point at the pressure P , and T_0 is the lower lambda point, which is taken to be 2.1720°K on the T^{58} scale.¹⁰ The 11 values reported by Elwell and Meyer³ are also shown. The solid line is calculated from an

equation of the form

$$(dP/dT)_\lambda = a_0 + a_1x + a_2x^2 + a_3x^3 + a_4 \exp(a_5x) \text{ atm/deg},$$

$$x = T_\lambda - T_0, \quad (1)$$

fitted to our data by the method of least squares. The values of the coefficients are given in Table I. The dashed line is calculated from the equation of Elwell and Meyer³:

$$(dP/dT)_\lambda = 86.7|x|^{0.342} - 120 \text{ atm/deg}. \quad (2)$$

Our results agree very well with those of Elwell and Meyer except at the highest temperatures. The 35-

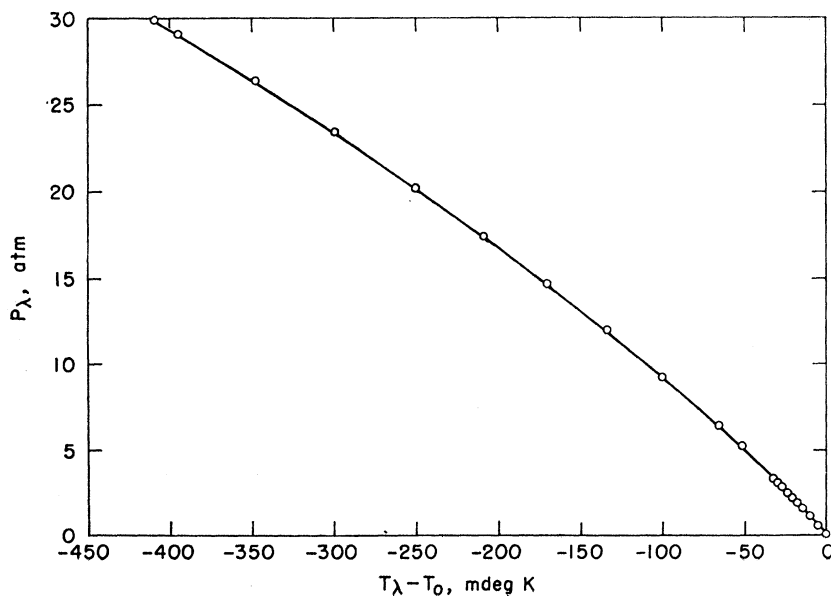


FIG. 5. Lambda pressures; \circ measured pressures. Solid line represents Eq. (3).

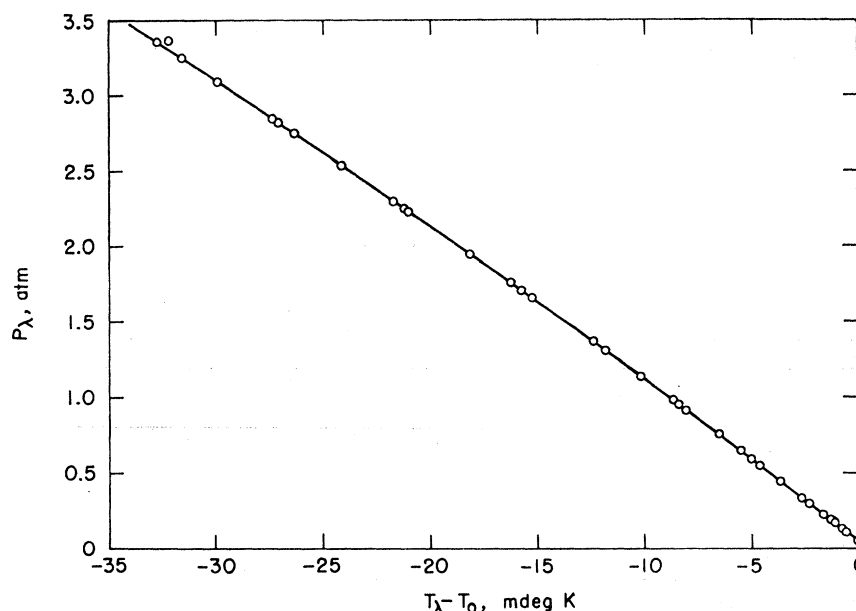


FIG. 6. Lambda pressures near the lower lambda point; \circ measured pressures. Solid line represents Eq. (3).

millidegree region just below the lower lambda point is shown in Fig. 4. Elwell and Meyer report only four values of $(dP/dT)_\lambda$ in this region, and these do not fit their curve very well. We suggest that the three-parameter Eq. (2) is inadequate to represent the whole of the lambda line and in particular that it has too large a curvature very near T_0 . Our measurements extrapolate rather smoothly to -111.05 ± 0.10 atm/deg at T_0 , compared to Elwell and Meyer's limiting slope of -120 ± 10 atm/deg. If Eq. (2) is disregarded, Elwell and Meyer's seven pressure measurements below 0.2 atm can be fitted very well with a straight line of slope -114 atm/deg.

Our observations of the lambda pressure are plotted in Fig. 5. Many points near the lower lambda point have been omitted for the sake of clarity. This region is shown in more detail in Fig. 6. The line is the integral of Eq. (1), and therefore has the form

$$P_\lambda = b_0 + b_1x + b_2x^2 + b_3x^3 + b_4x^4 + b_5 \exp(b_6x) \text{ atm.} \quad (3)$$

The values of the coefficients, which, except for b_0 , can be calculated from those of Eq. (1), are given in Table I. The value of b_0 was chosen so that the pressure at the lower lambda point is 0.04974 atm, to agree with the T_{58} temperature scale. The integral of Eq. (2), namely,

$$P_\lambda = 0.04974 - 120x - 64.60|x|^{1.342} \text{ atm,} \quad (4)$$

is hardly distinguishable from (3) on the scale of Figs. 5 and 6.

To facilitate comparison with lambda-pressure measurements by other observers, in Fig. 7 we have plotted $P_\lambda - P_e$, where P_e is the pressure calculated from Eq. (3). For the solid curve, P_λ was calculated from Eq. (4). For the dashed curve, P_λ was calculated from the cubic

equation of Lounasmaa and Kaunisto.¹¹ The plotted points represent our measurements and those of Elwell and Meyer,³ Lounasmaa and Kaunisto,¹¹ Vignos and Fairbank,¹² Swenson,¹³ Keller and Hammel,¹⁴ Grilly,¹⁵ and Grilly and Mills.¹⁶ The 35-mdeg range just below T_0 is shown similarly in Fig. 8.

The very close fit of our lambda pressures to Eq. (3) above $x = -35$ mdeg is to be expected since, in this region, the derivatives $(dP/dT)_\lambda$, from which (3) is derived, were measured with the same pressure gauge as were the absolute pressures. At lower temperatures the absolute pressures were measured with the stainless-steel Bourdon gauge, while the derivatives were measured with the quartz Bourdon gauge. As can be

TABLE I. Coefficients of equations for P_λ , ρ_λ , $(dP/dT)_\lambda$, and $(d\rho/dT)_\lambda$.

Property	1 $(dP/dT)_\lambda$ (atm/deg) a_n	3 P_λ (atm) b_n	5 $(d\rho/dT)_\lambda$ (mg/cm ³ deg) c_n	6 ρ_λ (g/cm ³) d_n
0	-95.0719	0.42800749	-150.735	0.14841388
1	-172.834	-95.0719	-659.645	-0.150735
2	-310.023	-86.417	-1590.94	-0.3298225
3	-310.087	-103.341	-1532.14	-0.53031333
4	-15.9822	-77.52175	-83.1635	-0.383035
5	42.2507	-0.37827065	36.7348	-0.00226388
6		42.2507		36.7348

¹¹ O. V. Lounasmaa and L. Kaunisto, Ann. Acad. Sci. Fennicae, Ser. AVI, No. 59 (1960).

¹² J. H. Vignos and H. A. Fairbank, Phys. Rev. **147**, 185 (1966).

¹³ C. A. Swenson, Phys. Rev. **89**, 538 (1953).

¹⁴ W. E. Keller and E. F. Hammel, Ann. Phys. (N. Y.) **10**, 202 (1960).

¹⁵ E. R. Grilly, Phys. Rev. **149**, 97 (1966).

¹⁶ E. R. Grilly and R. L. Mills, Ann. Phys. (N. Y.) **18**, 250 (1962).

seen in Figs. 5 and 7, the absolute pressures are larger than the calculated ones by about 0.14 atm, which is much larger than the reading error. It appears that the stainless-steel Bourdon gauge must have shifted by about 2 lb/in.² between the experiment and the gauge calibration. It is noteworthy that the pressures of Vignos and Fairbank,¹² who also used a Heise gauge, are likewise high. We have accepted the calculated pressures as correct since they are consistent with the measured derivatives and are based on measurements with the quartz Bourdon gauge, which cannot shift its calibration in this way. Furthermore, the calculated pressures are close to the mean of the various observa-

tions plotted in Fig. 7, and agree well with the careful work of Grilly.¹⁵

Swenson's measurements¹³ are generally 0.3 to 0.4 atm lower than the other measurements. This may be partly due to errors in his temperature scale. An error of 1 mdeg in temperature is equivalent to 0.05 to 0.10 atm in pressure.

In Fig. 8 are plotted all the data which might be used to determine the limiting slope $(dP/dT)_\lambda$ at the lower lambda point. Elwell and Meyer's equation indicates a slope more negative than ours, but their measured pressures closest to T_0 are quite consistent with ours. The work of Keller and Hammel has been

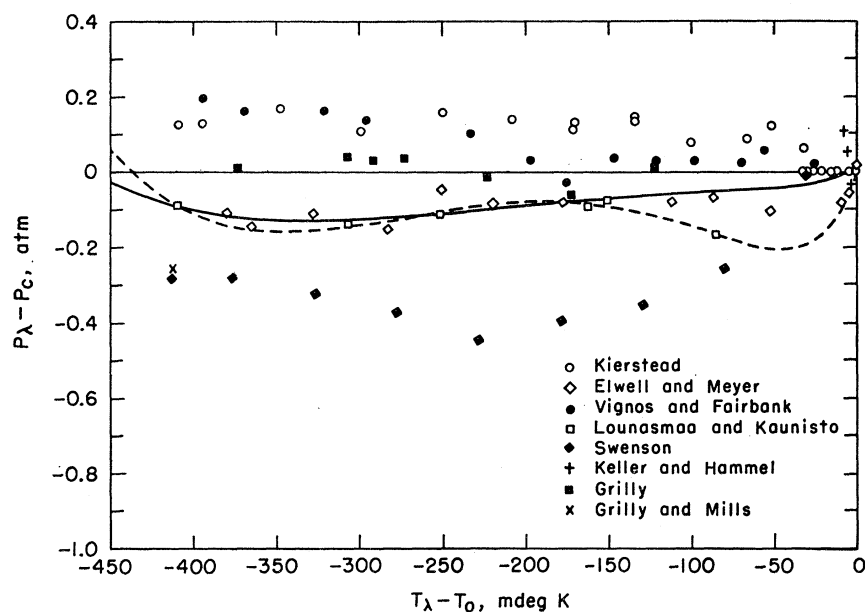


FIG. 7. Deviation of lambda pressures from Eq. (3). Solid line represents Eq. (4); dashed line represents Lounasmaa and Kaunisto's equation.

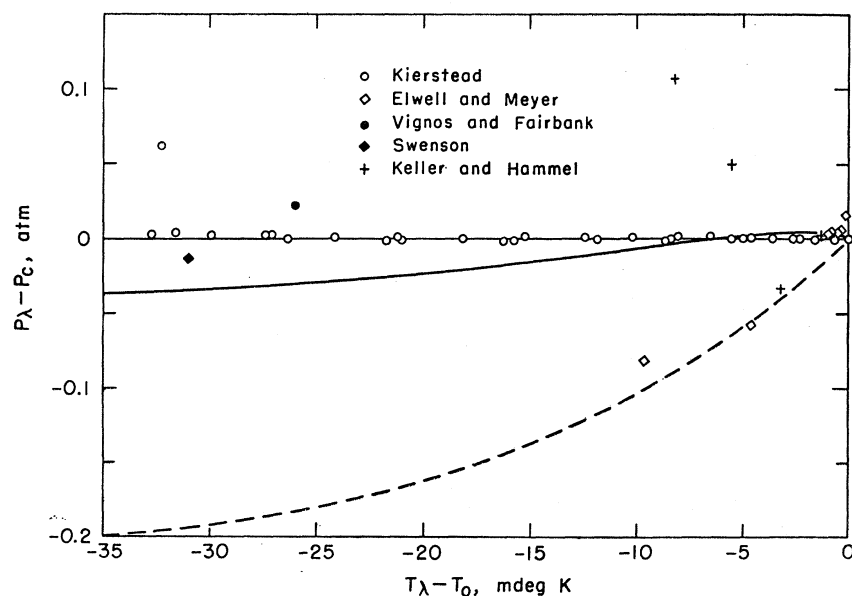


FIG. 8. Deviation of lambda pressures from Eq. (3) near the lower lambda point. Solid line represents Eq. (4); dashed line represents Lounasmaa and Kaunisto's equation.

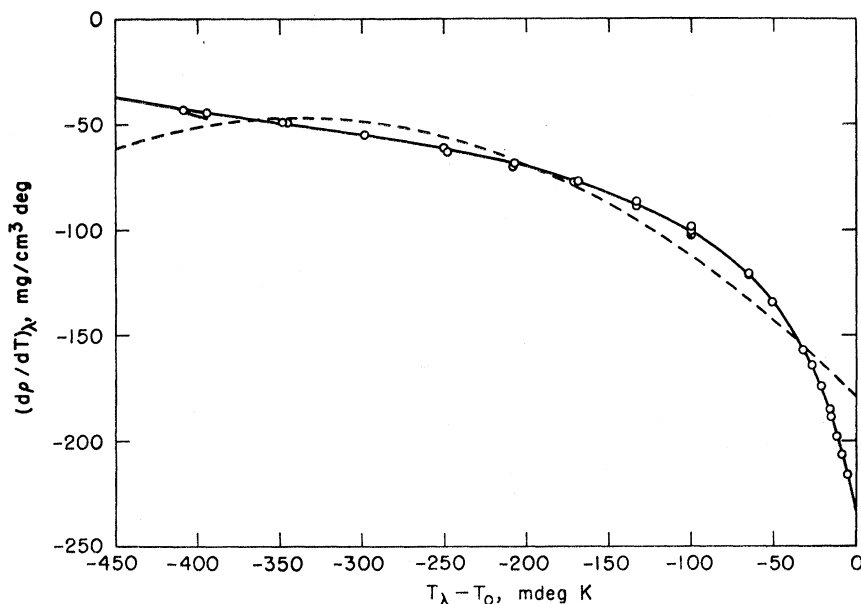


FIG. 9. Derivative $(d\rho/dT)_\lambda$ of the lambda line. \circ measured values. Solid line represents Eq. (5); dashed line represents Lounasmaa and Kaunisto's equation; short line at upper left represents our earlier work (Ref. 4).

quoted² to support a slope near -130 atm/deg, but, considering the scatter of the points, they are not inconsistent with a slope near -110 atm/deg. Lounasmaa and Kaunisto's equation gives a slope of -97.8 atm/deg, but this should not be taken seriously since their closest data point is 85 mdeg below T_0 .

IV. LAMBDA DENSITIES

As was mentioned earlier, because of the nature of our apparatus, we were able to measure $(d\rho/dP)_\lambda$ more accurately than $(d\rho/dT)_\lambda$. Therefore, $(d\rho/dT)_\lambda$ was calculated from the measured values of $(d\rho/dP)_\lambda$ and values of $(dP/dT)_\lambda$ calculated from Eq. (1). These values of $(d\rho/dT)_\lambda$ are plotted in Fig. 9. The solid line represents the equation

$$(d\rho/dT)_\lambda = c_0 + c_1x + c_2x^2 + c_3x^3 + c_4 \exp(c_5x) \text{ mg/cm}^3 \text{ deg}, \quad (5)$$

fitted to the data by the method of least squares. The values of the coefficients are given in Table I. The dashed line represents the derivative of Lounasmaa and Kaunisto's¹¹ cubic equation for ρ . The short line near the upper lambda point represents our earlier measurements⁴ in this region.

Although Lounasmaa and Kaunisto's curve agrees generally with ours, it has too little curvature at high temperatures and too much at low temperatures, with a maximum at 337 mdeg below T_0 (as has been pointed out by Goldstein).¹⁷

Our limiting slope of -233.9 ± 1.1 mg/cm³ deg at the lower lambda point involves some extrapolation, since we were unable to make accurate density measurements closer than 5 mdeg from T_0 . Elwell and Meyer,³ whose

¹⁷ L. Goldstein, Phys. Rev. **135**, A1471 (1964).

measurements extend to within 1 mdeg of the lower lambda point, find a limiting slope of -240 ± 7 mg/cm³ deg. The closest measurement of Lounasmaa and Kaunisto was 85 mdeg below T_0 , so the limiting slope of -179.3 mg/cm³ deg, calculated from their equation, is meaningless.

The integral of Eq. (5), namely,

$$\rho_\lambda = d_0 + d_1x + d_2x^2 + d_3x^3 + d_4x^4 + d_5 \exp(d_6x) \text{ g/cm}^3, \quad (6)$$

with the coefficients listed in Table I, is plotted as the solid line in Fig. 10. The dashed line represents Lounasmaa and Kaunisto's¹¹ cubic equation, and the plotted points represent experimental measurements of ρ_λ by Elwell and Meyer,³ Lounasmaa, and Kaunisto,¹¹ Lounasmaa and Kojo,¹⁸ Grilly and Mills,¹⁶ Edwards,¹⁹ Kerr,²⁰ and Kerr and Taylor.²¹ Figure 11 shows the 35-mdeg region just below the lower lambda point. The integration constant of Eq. (6) has been chosen to make ρ_λ agree with the measurement of Kerr and Taylor²¹ at the lower lambda point (0.14615 g/cm³). With this normalization, our curve passes within ± 0.0003 g/cm³ of most of the measurements.

V. LOWER AND UPPER LAMBDA POINTS

The lambda transformation was observed with the liquid in equilibrium with vapor, in both the sample compartment and the vapor-pressure compartment. The temperatures were the same to within 3 μ deg, and

¹⁸ O. V. Lounasmaa and E. Kojo, Ann. Acad. Sci. Fennicae Ser. A VI, No. 36 (1959).

¹⁹ M. H. Edwards, Can. J. Phys. **36**, 884 (1958).

²⁰ E. C. Kerr, J. Chem. Phys. **26**, 511 (1957).

²¹ E. C. Kerr and R. D. Taylor, Ann. Phys. (N. Y.) **26**, 292 (1964).

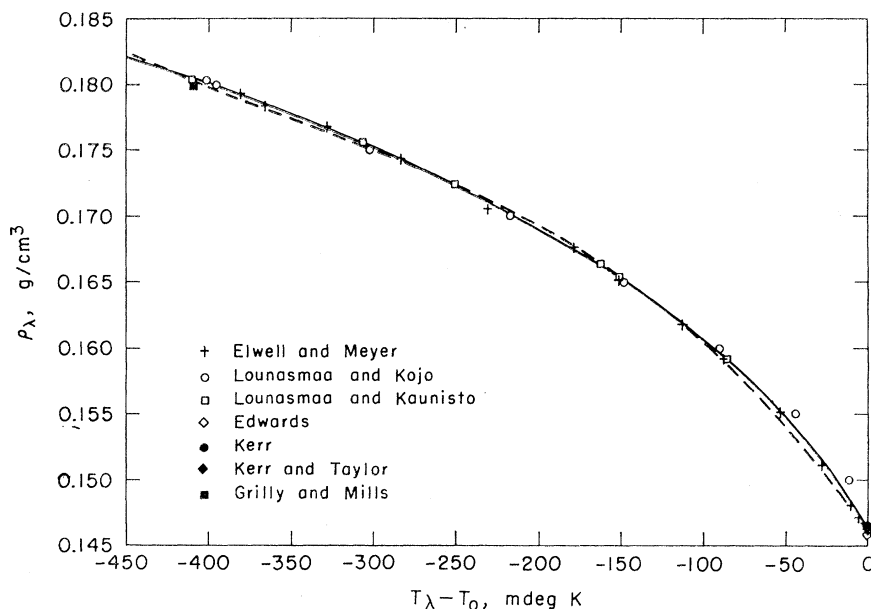


FIG. 10. Lambda densities. Solid line represents Eq. (6); dashed line represents Lounasmaa and Kaunisto's equation.

agreed with the value of 2.1720°K given for the lower lambda point in the T_{58} temperature scale¹⁰ to better than 0.1 mdeg. The tubes to the vapor-pressure compartment were more suitable for measuring a very small pressure, and the pressure observed in this compartment was 0.04974 atm, agreeing with the T_{58} scale to within 10^{-5} atm.

The upper lambda temperature, observed with solid and liquid in equilibrium in the sample compartment, was $1.7633 \pm 0.0001^\circ\text{K}$, in agreement with our previous determinations.^{4,5} The pressure calculated for this

temperature using Eq. (3) is 29.74 ± 0.05 atm, and the density calculated using Eq. (6) is 0.18044 ± 0.00030 g/cm³. The properties of the upper and lower lambda points are listed in Tables II and III, together with those reported by other investigators.

There is good agreement among the various workers on the temperature, pressure, and density of the lower lambda point. At the upper lambda point there is fairly good agreement on the temperature and density. Our present value for the pressure is in good agreement with those of Grilly and Mills and of Lounasmaa and

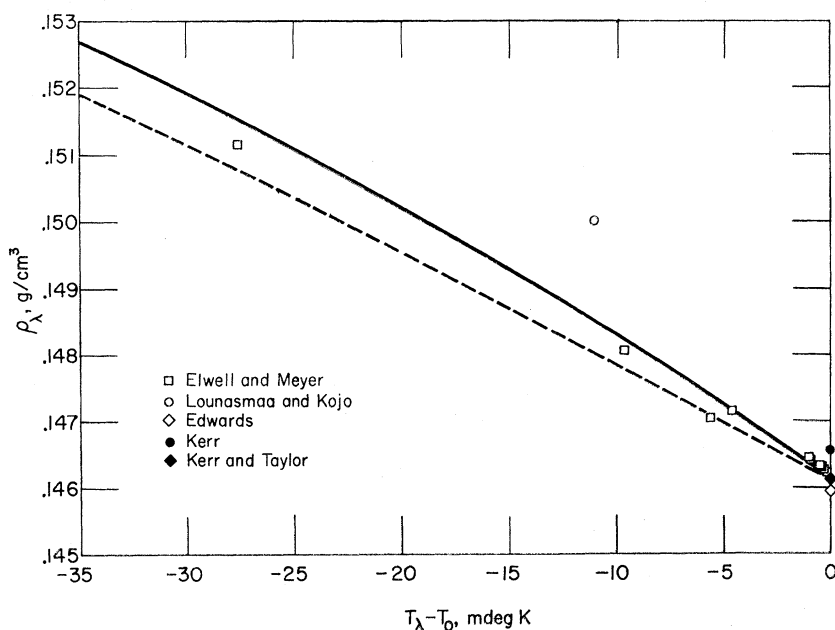


FIG. 11. Lambda densities near the lower lambda point. Solid line represents Eq. (6); dashed line represents Lounasmaa and Kaunisto's equation.

TABLE II. Properties of the lower lambda point.

	Temperature (°K)	Pressure (atm)	Density (g/cm ³)	$(dP/dT)_\lambda$ (atm/deg)	$(d\rho/dT)_\lambda$ (mg/cm ³ deg)
Lower lambda point					
This work	2.1720±0.0001	0.04974±0.00001	0.14615 ^f	-111.05±0.10	-233.9±1.1
T_{68} scale ^a	2.1720	0.04974			
Edwards ^b	2.1728		0.14596		
Kerr ^c	2.172		0.14657		
Kerr and Taylor ^d	2.1720		0.14615		
Elwell and Meyer ^e	2.172 ±0.001	0.0497 ±0.0001		-120 ±10	-240 ±7

^a Reference 10.^b Reference 19.^c Reference 20.^d Reference 21.^e Reference 3.^f Adopted value.

TABLE III. Properties of the upper lambda point.

	Temperature (°K)	Pressures (atm)	Density (g/cm ³)	$(dP/dT)_\lambda$ (atm/deg)	$(d\rho/dT)_\lambda$ (mg/cm ³ deg)
Upper lambda point					
This work	1.7633±0.0001	29.74±0.05	0.18044±0.00030	-55.05±0.50	-42.3±0.5
Kierstead ^a	1.7633±0.0001	29.84±0.02		-55.5 ±1.0	-43.7±1.5
Kierstead ^b	1.7632±0.0001	29.83±0.02			
Ahlers ^c	1.763 ±0.001				
Grilly and Mills ^d	1.760 ±0.001	29.67±0.01	0.17989		
Vignos and Fairbank ^e	1.765 ±0.003	29.90±0.05			
Lounasmaa and Kaunisto ^f	1.762 ±0.001	29.71±0.01	0.1803	-57.4	-53.05
Swenson ^g	1.760 ±0.003	29.64±0.03		-54.5	
Edwards and Pandorf ^h	1.763 ±0.002				

^a Reference 4.^b Reference 5.^c G. Ahlers, Phys. Rev. **135**, A10 (1964).^d Reference 16.^e Reference 12.^f Reference 11.^g Reference 13.^h D. O. Edwards and R. C. Pandorf, Phys. Rev. **144**, 143 (1966).

Kaunisto. Our earlier measurement and that of Vignos and Fairbank were made with metal Bourdon gauges, and both are too high. The probable error assigned in our earlier papers^{4,5} did not include an allowance for possible zero shifts, and should be increased to about 0.2 atm. The measurement of Swenson is a little low, as are all his lambda pressures. Our measurement of $(dP/dT)_\lambda$ agrees with our previous measurement and with that of Swenson, while our $(d\rho/dT)_\lambda$ is in reasonable agreement with our previous value. Slopes calculated from Lounasmaa and Kaunisto's pressure and density equations deviate considerably since the equations are based on too few measured points to be differentiated accurately.

VI. CONCLUSION

Equations (3) and (6) represent the pressure and density of the lambda curve as a function of tempera-

ture to within 0.05 atm and 0.003 g/cm³, respectively. They can be differentiated [yielding Eqs. (1) and (5)] to give $(dP/dT)_\lambda$ to a few tenths of an atm/deg and $(d\rho/dT)_\lambda$ to 1 mg/cm³ deg anywhere on the lambda line. The exponential term was found to be essential to obtain a good fit to the high curvature near T_0 and the nearly linear portion at lower temperatures. No theoretical significance is attached to this form.

Our measurements agree generally with previous work on the lambda curve, but we believe they represent a higher order of accuracy and detail, particularly with regard to the derivatives.

ACKNOWLEDGMENTS

We wish to express our thanks to David Elwell and Professor Horst Meyer of Duke University for making their numerical results available to us in advance of publication.